Journal of Thermal Analysis and Calorimetry (2023) 148:3129–3135
https://doi.org/10.1007/s10973-022-11382-9

Numerical simulation of a modified trapped vortex combustor

Dharsannen Sri Selvam[1] · Norwazan Abdul Rahim[1] · Mohd Rashdan Saad[1] · Syahar Syawal[2] · Hasan Mohd Faizal[3] · Mohd Rosdzimin Abdul Rahman[1]

Received: 19 January 2022 / Accepted: 25 April 2022 / Published online: 30 May 2022

Abstract
Analysing the flow inside the combustor is important for determining the performance and NOx emission of the combustors. This study investigated combustion and flow characteristics inside a modified trapped vortex combustor (TVC) to enhance the performance and reduce the NOx emission. The modified TVC was characterised by a variable guide vane ratio between length of column guide vane inside cavity and height of the cavity. The effect of the incoming velocity was analysed. The Arrhenius rate of the one-step methane/air reaction mechanism was used. Validation of the study results was performed by comparing the present numerical results with the published experimental results. Numerical results demonstrated significant changes in the vortex inside the cavity after introducing the guide vane. Furthermore, variable guide vane ratio was found to have a significant effect on temperature, NOx emission, and combustion efficiency with reduction of 5, 90, and 2%, respectively, at guide vane ratio 0.75. The guide vane ratio of 0.5 was found to be the cutoff design for the current TVC model. Increasing the guide vane ratio larger than 0.5 was found to reduce the NOx emission but needed to compensate with drop of the combustion efficiency. This study has improved the understanding of the effect of the guide vane on the development of a high-efficiency low-NOx TVC.

Keywords Combustion · Trapped vortex combustor · Inlet vane · Numerical simulation

Introduction

Low-NOx combustors have been widely used in various applications such as in aero engines and modern gas turbines. A wide range of combustor designs have been developed to operate at high efficiency and produce low NOx emission [1]. One of the most remarkable combustors is the trapped vortex combustor (TVC), which generally uses a cavity to stabilise the flame. A more recent TVC is the advanced trapped vortex combustor (AVC) [1–7], which uses bluff bodies instead of cavities [4–9]. These bluff bodies are arranged at the front and rear sections of the combustion chamber, and the cavity of combustor is located in between front and rear bluff bodies. The bluff body is known to have considerable importance effect on the flow separation and plays a vital role in enhancing the fuel mixing. As the incoming air flows into the front bluff body, a strong vortex circulation is produced between front and rear bluff bodies. This produces a stable ignition source inside the combustion chamber.

In the last few years, the technology of TVC has been increasingly focused on efficient combustion and reduced emissions [9]. Operating the combustor at lean fuel/air regime is quite a challenge because a small change in the incoming flow may lead to combustion instability [10]. Nowadays, TVCs are devised so as to overcome the difficulties that may arise because of the use of cavity for stabilising pilot flame. TVC is an advanced combustor based on the conventional swirl-stabilised designs used for the past 60 years in gas turbine combustors. It uses the physical wall cavity to create recirculation zones for flame stabilisation and radial combustion phases [10]. A dual counter-rotating vortex can be formed and securely locked in the cavity when

✉ Mohd Rosdzimin Abdul Rahman
rosdzimin@gmail.com

[1] Department of Mechanical Engineering, Faculty of Engineering, Universiti Pertahanan Nasional Malaysia, Kem Sg Besi, Kuala Lumpur, Malaysia

[2] School of Mechanical Engineering, College of Engineering, Universiti Teknologi MARA, Shah Alam, Malaysia

[3] Automotive Development Centre, Institute for Vehicle System and Engineering, Universiti Teknologi Malaysia, 81310 Baharu, Johor, Malaysia

the TVC cavity size is well built [11]. This allows for stable combustion and does not reveal the flow of the stream. Edmonds et al. [3] developed a new design of AVC and showed that the oscillation of the flame is eliminated and the pressure loss is reduced. Deng et al. [12] conducted a study on AVC by using hydrogen as a fuel and found that the total pressure loss and combustion efficiency are affected by the equivalent ratio. Zeng et al. [13] investigated the effect of slot in the rear blunt body and showed that the performance of the AVC could be increased when the slot size and opening angle are matching. Xie and Zhu [8] proposed a modified AVC configuration by changing the external structure of the combustor. They found that the pollutants emissions, pressure drop, and combustion efficiency are significantly affected by the proposed model. Wang et al. [14] studied the effect of guide vanes to AVC numerically and reported the existence of a double-vortex structure. Han et al. [15] studied high-temperature corrosion after low NOx transformation using modified air flow inside the burner and observed that the proper arrangement of the burner will reduce the corrosion and NOx. Enhancement of the mixing due to effect of swirling on the TVC was studied by Jin et al. [16]. However, the data on the combustion stability and efficiency have not been not provided by the authors. Moreover, Sun et al. [17] investigated the effect of jet arrangement on the TVC with inverse diffusion combustion and found that multi-jet is better for combustion performance when the jet arranged in the same position. The emission of NOx was not taken into consideration by the authors [17].

Guide vanes are useful as they create a double vortex, which has a number of advantages [18, 19]. Zeng et al. [18] studied several ratios of the guide vane. In the present study, the ratio between length of the column inside the cavity and height of the cavity was investigated. The rationale behind this configuration is to increase the vortex formation inside the cavity to enhance the mixing and anchoring the flame.

Numerical work

Figure 1 illustrates the computational model of a two-dimensional TVC with a guide vane. Herein, a is the length of column guide vane inside the cavity, with combustor inlet height, $H = 0.02$ m, length of combustor, $L = 0.2$ m, length from cavity to outlet, $W = 0.1$ m, cavity height, $h = 0.03$ m, height of mainstream inlet vane, $b = 0.002$ m, and the guide vane has a thickness of 0.001 m. It was designed in accordance with experimental and numerical investigation on microcombustor with a bluff-body carried out by Wang et al. [14]. Guide vane ratio is defined as length of column guide vane inside the cavity to height of the cavity, a/h.

For simulations, Ansys Fluent, a commercial computational fluid dynamics software, was used in the present study.

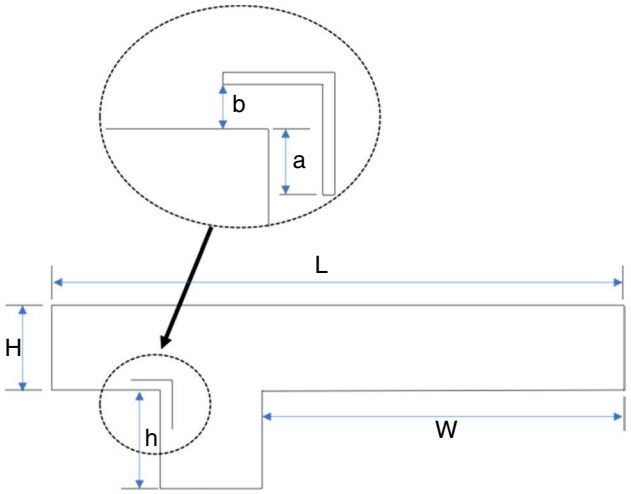

Fig. 1 Computational domain

The finite volume approach was used to solve the conservation equations. The conservation equations of mass, momentum, and energy are as follows:

Conservation equation of mass:

$$\nabla \cdot \left(\rho \vec{v}\right) = 0 \tag{1}$$

Conservation equation of momentum:

$$\nabla \cdot \left(\rho \vec{v}\vec{v}\right) = -\nabla p + \nabla \cdot \left(\overline{\tau}\right) \tag{2}$$

Conservation equation of energy:

$$\nabla \cdot \left(\vec{v}(\rho E + p)\right) = -\nabla\left(K_{\text{eff}}\nabla T - \sum_i h_i \vec{j}_i + \left(\overline{\tau_{\text{eff}}} \cdot \vec{v}\right)\right) + S_{\text{E}} \tag{3}$$

where ρ is the density, v is the velocity, p is the static pressure, τ is the stress tensor, E is the total energy, K is the thermal conductivity, h is enthalpy, J is the diffusion flux of species, and S_{E} is the heat source term.

The turbulence model used in the present study is the realisable $k - \varepsilon$ model. The model equations are as follows:

$$\frac{\partial}{\partial t}(\rho k) + \frac{\partial\left(\rho k u_{\text{j}}\right)}{\partial x_{\text{j}}} = \frac{\partial}{\partial x_{\text{j}}}\left[\left(\mu + \frac{\mu_{\text{t}}}{\sigma_{\text{k}}}\right)\frac{\partial k}{\partial x_{\text{j}}}\right] + G_{\text{k}} - \rho\varepsilon \tag{4}$$

$$\frac{\partial}{\partial t}(\rho\varepsilon) + \frac{\partial\left(\rho\varepsilon u_{\text{j}}\right)}{\partial x_{\text{j}}} = \frac{\partial}{\partial x_{\text{j}}}\left[\left(\mu + \frac{\mu_{\text{t}}}{\sigma_{\varepsilon}}\right)\frac{\partial \varepsilon}{\partial x_{\text{j}}}\right] + \rho C_1 S_{\varepsilon} - \rho C_2 \frac{\varepsilon^2}{k + \sqrt{\nu\varepsilon}} \tag{5}$$

where k is the turbulence kinetic energy, ε is the dissipation rate, G is the turbulence kinetic energy generation, C_1 and C_2 are constant, and σ is the turbulent Prandtl number.

The SIMPLE algorithm was used to solve the pressure–velocity coupling. The convergence criterion was set as 10^{-5} for energy equation. The velocity boundary condition was used for methane/air mixture at the inlet with the temperature of 300 K, the pressure outlet boundary condition was set for the combustor outlet, and the combustor wall boundary condition was considered no-slip and adiabatic. Kinetic theory was used to estimate the transport properties. The heat conductivity and viscosity for particular species, and ideal gas mixing law were used to calculate the mixture of the transport properties. An ideal gas law assumption was used to calculate the specific heat. The k–ε model was used in this study. The k–ε model has been shown to have a higher accuracy compared to large eddy simulation (LES) model [20]. The air is assumed to be a mixture of O_2 and N_2 with 21 mol% and 79 mol%, respectively. The methane/air combustion elements are very complicated and involve hundreds of interaction particles among gas species and thus require long computation times. In this study, only one-step reaction mechanism of methane/air was used because it is good enough to analyse the flame dynamics according to Westbrook and Dryer [21], and therefore, detailed chemical reaction is not required. The model was simulated as methane single-step oxidation with oxygen where the products are water vapor and carbon dioxide. The equivalence equation is as follows:

$$CH_4 + 2O_2 \rightarrow CO_2 + 2H_2O \tag{6}$$

The reaction rate used is the global one-step methane oxidation reaction rate or the Arrhenius-type reaction rate model introduced by Westbrook and Dryer [21]. The Arrhenius reaction rate was coupled with the eddy dissipation model to tackle the turbulence. The Arrhenius-type reaction rate model equation is as follows:

$$r_{CH4} = 1.3 \times 10^8 \exp\left(-2.027 \times 10^8/RT\right) \times \left[CH_4\right]^{0.2}\left[O_2\right]^{1.3} \tag{7}$$

Results and discussion

Mesh dependency test was conducted successfully on the model, and the data are presented in Fig. 2. To save the computational time, only half domain of the combustor was adopted, and the structured hexahedral meshes were generated. The velocity magnitude comparison at outlet with different grids is shown in Fig. 2. The result with the mesh size 0.0005 m and 0.001 m is in significant agreement. To reduce the computation time, the grid with mesh size 0.001 m was selected in this study.

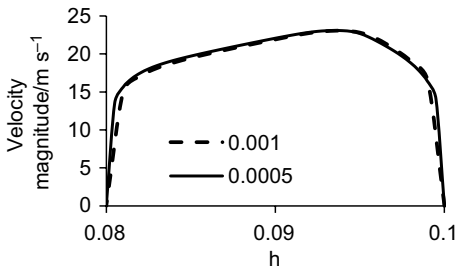

Fig. 2 Velocity at outlet

Numerical validation

Validation of the numerical model and reaction mechanism of the methane/air non-premixed combustion was carried out by comparing with the experimental data [22]. Validation was performed according to the total pressure loss coefficient as shown below:

$$\delta^* = \left(P^*_{\text{inlet}} - P^*_{\text{outlet}}\right)/P^*_{\text{inlet}} \tag{8}$$

where P^*_{inlet} denotes the total pressure at the inlet, while P^*_{outlet} denotes the total pressure at the outlet. The comparison between numerical simulation and experimental approach for total pressure loss is depicted in Fig. 3, which shows that the numerical simulation results are in agreement with the experimental results. A minor discrepancy seen in Fig. 3 is attributable to simplified reaction model used in the present study. This validation showed that the present numerical method is acceptable.

The velocity magnitude at the outlet is observed with guide vane ratios of 0.1, 0.25, 0.5, and 0.75 are shown in Fig. 4. The outlet velocity magnitude was relatively the same for all guide vane ratios for the inlet velocity of 20 m s^{-1}, 40 m s^{-1}, and 50 m s^{-1} with 72 m s^{-1}, 126 m s^{-1}, and 145 m s^{-1}, respectively. Furthermore, the inlet velocity of 50 m s^{-1} gave the highest outlet velocities for all four types of guide vanes. These observations are presented in Fig. 3. Higher inlet velocity produced higher total pressure loss coefficient.

Figure 5 shows the total temperature distribution at the outlet for different guide vane ratios and inlet velocities. The temperature distribution at outlet slightly changed because of different guide vane ratios. Temperature of 20 m s^{-1} inlet velocity case was found to have the highest outlet temperature at 1672 K, while the 40 m/s inlet velocity case gave the lowest temperature of 1415 K at guide vane ratio = 0.75. Interestingly, at guide vane ratio = 0.5, increase in the guide vane ratio decreased the outlet temperature. This trend was observed for all inlet velocity cases in the present study.

Figure 6 illustrates the emissions of NOx according to four different ratios of guide vane. The trendline for NOx emission varies greatly in all four guide vane ratios. It was

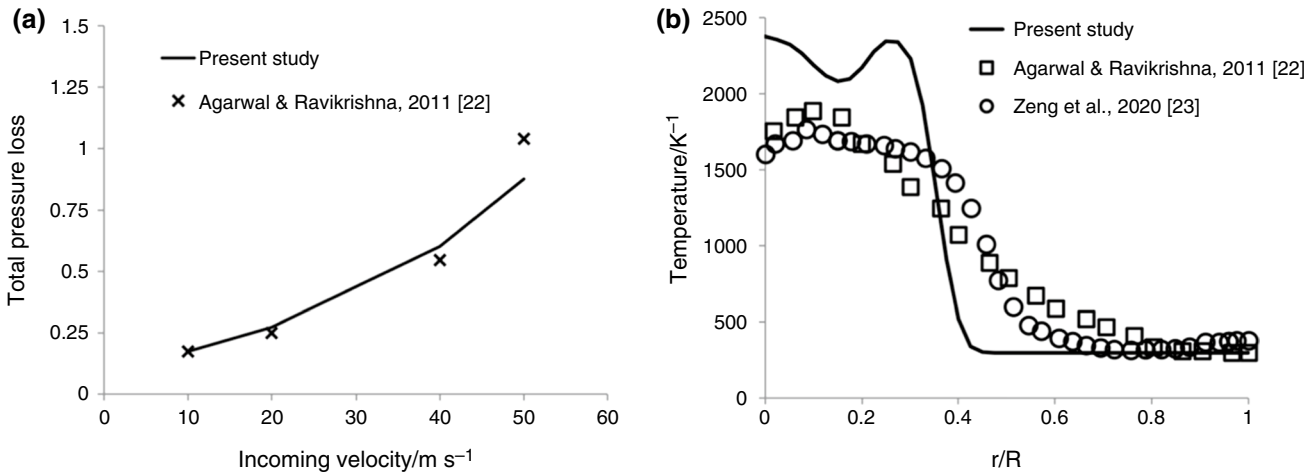

Fig. 3 Validation of present simulation work and published experimental approach by Agarwal and Ravikrishna [22] and Zeng et al. [23] of **a** total pressure loss and **b** temperature at the outlet

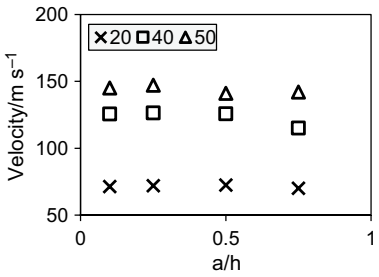

Fig. 4 Velocity of the outlet at various inlet velocity values and guide vane ratios

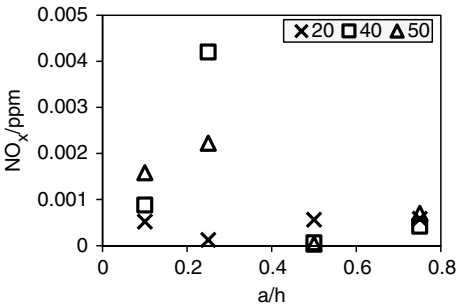

Fig. 6 Emission of NOx at the outlet

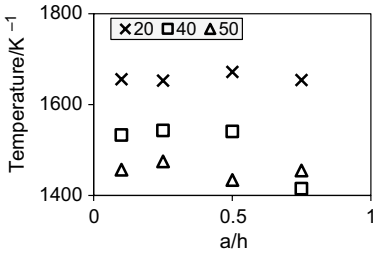

Fig. 5 Temperature of the outlet at various inlet velocity and guide vane ratio

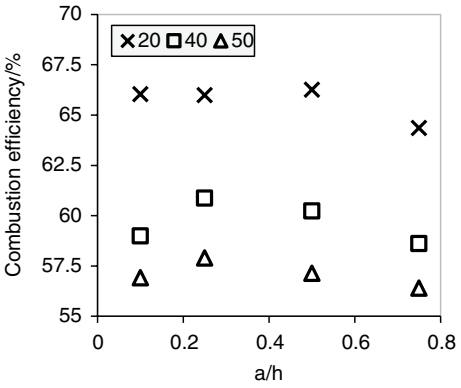

Fig. 7 Combustion efficiency

found that the ratio of guide vane significantly affected the emission of NOx. At inlet velocity of 20 m s^{-1}, the emission NOx decreased with increase in guide vane ratio. Unfortunately, at guide vane ratio = 0.5 the NOx emission increased gradually. At inlet velocity of 40 m s^{-1} and 50 m s^{-1}, trend of the NOx emission was found to be similar. NOx emission increased sharply at guide vane ratio of 0.25. Later, at guide vane ratio = 0.5, NOx emission dropped about 90% for 40 m s^{-1} case and increased at guide vane ratio = 0.75. Therefore, selection of the guide vane ratio needs to be conducted carefully because of the significant effect on the emission of NOx.

Figure 7 shows the combustion efficiency for all four types of guide vane ratios for inlet velocities of 20 m s^{-1},

40 m s^{-1}, and 50 m s^{-1}. Combustion rate was determined with the mass fraction of methane entering and exiting the combustor. The equation to evaluate the combustion efficiency is as follows:

$$\text{Combustion Efficiency} = \left(\frac{Y_{\text{in}} - Y_{\text{out}}}{Y_{\text{in}}}\right)100 \quad (9)$$

Inlet velocity of 20 m s^{-1} had high combustion rate with the combustion efficiency above 65% compared to 40 m s^{-1} and 50 m s^{-1}. This is attributable to slow speed of fluid flow at which the combustion rate of methane and oxygen is higher. Hence, inlet velocity of 40 m s^{-1} had higher combustion efficiency of 60% compared to 57% for 50 m s^{-1}. In general, increase in inlet velocity reduces the combustion efficiency. This finding corresponds to the observations by Xie and Zhu [8], who assumed reduction in combustion efficiency to be due to the increase in the total pressure loss.

When the TVC was operated with the addition of guide vane in the mainstream, there was a significant alteration inside the cavity. The velocity of the cavity flow increased with increase in guide vane ratio (Fig. 8). Moreover, cavity region grew with increase in guide vane ratio. This flow pattern is attributable to guided flow from the guide vane into the bottom of the cavity. Therefore, the velocity in the cavity increases and increases the momentum. This will enhance the turbulent motion that improve mixing of the fuel/air mixture. The phenomena will lead to higher level of uniformness of temperature distribution inside cavity. Thus, increase in the guide vane ratio increased the wall shear stress at the bottom, as discussed previously by Wang et al. [20].

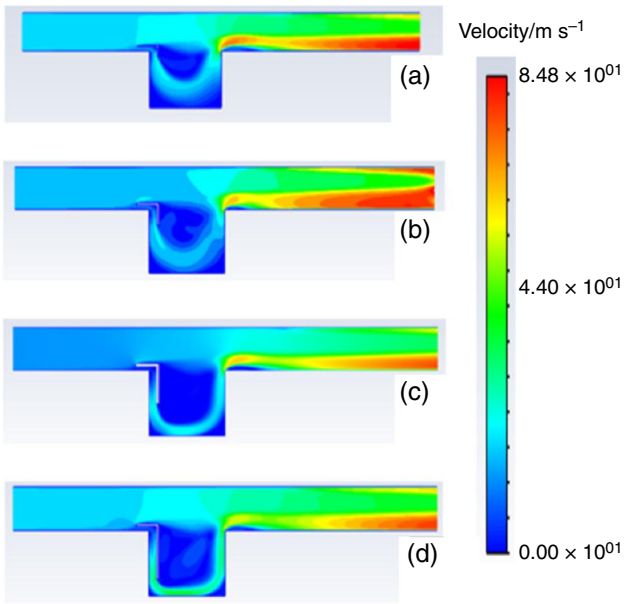

Fig. 8 Velocity contour for guide vane ratio **a** 0.1, (2) 0.25, (3) 0.5, and (4) 0.75 at inlet velocity of 20 m/s

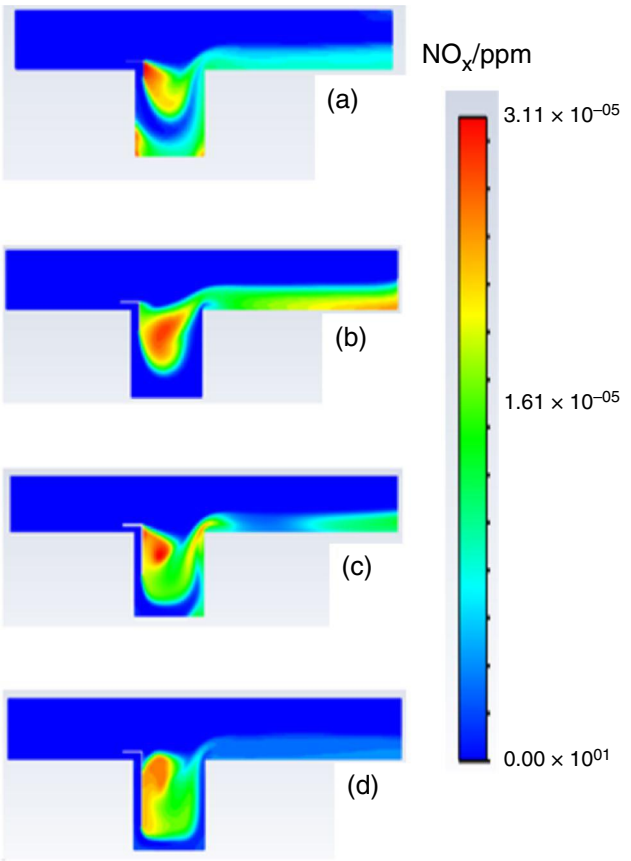

Fig. 9 Contour of the NOx emissions for guide vane ratio (1) 0.1, (2) 0.25, (3) 0.5, and (4) 0.75 at inlet velocity of 20 m s^{-1}

Figure 9 shows the emissions of NOx distribution for various guide vane ratios. At ratio 0.25, the highest amount of NOx is generated in the centre of the cavity because of the excessively unevenly temperature distribution and high local temperature.

At ratio 0.1 and 0.5, NOx emissions are slightly high. However, at ratio 0.75 the guide vane ratio relatively influences the emissions of NOx, where it contribute to lower NOx emissions. The main reason is the mixing region inside the cavity which is large and helps to increase the mixing rate and in turn reduce NOx emissions.

Conclusions

This study investigated the characteristics of the modified TVC model. The validation of numerical work agreed with published experimental work. The main conclusions are:

1. Ratio of the guide vane has less effects on the outflow velocity. At inlet velocity of 20 m s^{-1}, 40 m s^{-1}, and 50 m s^{-1}, the outlet velocity was noted to be consistent

at 72 m s^{-1}, 126 m s^{-1}, and 145 m s^{-1}, respectively, at various guide vane ratios.

2. Temperature and combustion efficiency are slightly affected at the guide vane ratio beyond 0.5. At inlet velocity of 40 m s^{-1}, the temperature and combustion efficiency dropped about 5% and 2%, respectively, for guide vane ratio of 0.75.
3. The NOx emission is significantly affected by the guide vane ratio. At guide vane ratio of 0.75, the NOx emission dropped 90% for the 40 m s^{-1} inlet velocity case.
4. The guide vane ratio of 0.5 is the cutoff design for the current TVC model. Beyond this value, the NOx showed a better reduction in emission, but the combustion efficiency dropped.
5. The proposed modified TVC showed a significant flow modification inside the combustor. This flow modification affected the characteristics of the combustor behaviour. The NOx reduction needed to compensate with drop in combustion efficiency for the application of the proposed TVC model.

Acknowledgements The authors would like to thanks the Universiti Pertahanan Nasional, Malaysia, for giving the full support in this research work.

Author contributions DSS contributed to writing–original draft preparation, conceptualisation, methodology, investigation; NAR contributed to writing–reviewing and editing, visualisation; MRS contributed to writing–reviewing and editing, visualisation; SS contributed to writing–reviewing and editing, visualisation; HMF contributed to writing–reviewing and editing, visualisation; and MRAR contributed to supervision, project administration, funding acquisition, writing–reviewing and editing.

References

1. Singh OK. Combustion simulation and emission control in natural gas fuelled combustor of gas turbine. J Therm Anal Calorim. 2016;125(2):949–57. https://doi.org/10.1007/s10973-016-5472-0.
2. Kendrick DW, Chenevert BC, Trueblood B, Tonouchi J, Lawlor SP, Steele R. Combustion system development for the ramgen engine. J Eng Gas Turbines Power. 2003;125(4):885–94. https://doi.org/10.1115/1.1586314.
3. Edmonds RG, Steele RC, Williams JT, Straub DL, Casleton KH, Bining A. Ultra-low NOx advanced vortex combustor. In Turbo Expo: Power Land Sea Air. 2006;42363:255–62. https://doi.org/10.1115/GT2006-90319.
4. Zhao D, Gutmark E, de Goey P. A review of cavity-based trapped vortex, ultra- compact, high-g, inter-turbine combustors. Prog Energy Combust Sci. 2018;66(1):42–82. https://doi.org/10.1016/j.pecs.2017.12.001.
5. Hsu KY, Goss LP, Roquemore WM. Characteristics of a trapped-vortex combustor introduction. J Propuls Power. 1998;14(1):57–65. https://doi.org/10.2514/2.5266.
6. Wan J, Fan A. Recent progress in flame stabilization technologies for combustion-based micro energy and power systems. Fuel. 2021;286: 119391. https://doi.org/10.1016/j.fuel.2020.119391.
7. Jiang B, Gaowei CUI, Yi JI, Ziqiang ZH, Dong LI, Xiaomin HE. Flow field characteristics, mixing and emissions performance of a lab-scale rich-quench-lean trapped-vortex combustor utilizing a quench orifice plate combined with a bluff-body. Chin J Aeronaut. 2021;34(4):476–92. https://doi.org/10.1016/j.cja.2020.08.030.
8. Xie J, Zhu Y. Characteristics study on a modified advanced vortex combustor. Energy. 2020;193:116805. https://doi.org/10.1016/j.energy.2019.116805.
9. Jiang B, Jin Y, Liu D, Wu Z, Ding G, Zhu Z, He X. Effects of multi-orifice configurations of the quench plate on mixing characteristics of the quench zone in an RQL-TVC model. Exp Therm Fluid Sci. 2017;83:57–68. https://doi.org/10.1016/j.expthermflusci.2016.12.011.
10. Kumar PE, Mishra DP. Flame stability characteristics of two-dimensional trapped vortex combustor. Combust Sci Technol. 2016;188(8):1283–302. https://doi.org/10.1080/00102202.2016.1190343.
11. Zeng Z, Du P, Wang ZK, Li K. Combustion flow in different advanced vortex combustors with/without vortex generator. Aero Sci Technol. 2019;86:640–9. https://doi.org/10.1016/j.ast.2019.01.048.
12. Deng Y, Jiang X, Su F. Combustion characteristics of advanced vortex combustor burning H_2 fuel. In: ASME International Mechanical Engineering Congress and Exposition; 2014:IMECE2014–37475. https://doi.org/10.1115/IMECE2014-37475
13. Zeng Z, Wang H, Wang Z. Analysis of cooling performance and combustion flow in advanced vortex combustor with guide vane. Aero Sci Technol. 2018;72:542–52. https://doi.org/10.1016/j.ast.2017.11.027.
14. Wang ZK, Zeng ZX, Li K, Xu YH. Effect of structure parameters of the flow guide vane on cold flow characteristics in trapped vortex combustor. J Hydrodyn. 2015;27(5):730–7. https://doi.org/10.1016/S1001-6058(15)60535-2.
15. Han B, Lin H, Miao Z. Numerical investigation on the optimized arrangement for high-temperature corrosion after low NOx transformation. J Therm Anal Calorim. 2021;146(5):2183–97. https://doi.org/10.1007/s10973-021-10734-1.
16. Jin Y, Zhang K, Yao K, Wang Y, He X. Effect of mainstream swirling on flowfield characteristics of an outer-cavity trapped vortex combustor. J Appl Fluid Mech. 2021;14(4):1183–94. https://doi.org/10.47176/JAFM.14.04.32262.
17. Sun H, Yan P, Tian L, Xu Y. Numerical simulation of inverse diffusion Combustion and flow characteristics in a trapped vortex combustor. Int J Aeronaut Space Sci. 2021;22(3):625–37. https://doi.org/10.1007/s42405-020-00335-x.
18. Zeng Z, Cheng H, Wang Z. Investigation of the flow and heat transfer characteristics in advanced vortex combustor. Int J Therm Scie. 2018;156: 106459. https://doi.org/10.1016/j.ijthermalsci.2020.106459.
19. Gao W, Yan Y, Shen K, Huang L, Zhao T, Gao B. Combustion characteristic of premixed H_2/air in the micro cavity combustor with guide vanes. Energy. 2022;239:121975. https://doi.org/10.1016/j.energy.2021.121975.
20. Razmjooei B, Ravangard AR, Momayez L, Ferchichi M. The influence of heat transfer due to radiation heat transfer from a combustion chamber. J Therm Anal Calorim. 2021. https://doi.org/10.1007/s10973-020-10263-3.
21. Westbrook CK, Dryer FL. Simplified reaction mechanisms for the oxidation of hydrocarbon fuels in flames. Combust Sci Technol. 1981;27(1–2):31–43. https://doi.org/10.1080/00102208108946970.

22. Agarwal KK, Ravikrishna RV. Experimental and numerical studies in a compact trapped vortex combustor: stability assessment and augmentation. Combust Sci Technol. 2011;183(12):1308–27. https://doi.org/10.1080/00102202.2011.592516.
23. Zeng Z, Guo K, Gong X. Combustion turbulence flow in trapped vortex combustor with guide vane and blunt body. Int J Aerosp Eng. 2020. https://doi.org/10.1155/2020/8882343.